



# Deep viewing for the identification of Covid-19 infection status from chest X-Ray image using CNN based architecture

Partho Ghose<sup>\*,a</sup>, Md. Ashraf Uddin<sup>a</sup>, Uzzal Kumar Acharjee<sup>a</sup>, Selina Sharmin<sup>a</sup>

Department of Computer Science and Engineering, Jagannath University, Dhaka, Bangladesh

## ARTICLE INFO

### Keywords:

Coronavirus (Covid-19)  
Classification  
Deep learning  
Chest x-ray  
Convolutional Neural Network (CNN)

## ABSTRACT

In recent years, coronavirus (Covid-19) has evolved into one of the world's leading life-threatening severe viral illnesses. A self-executing accord system might be a better option to stop Covid-19 from spreading due to its quick diagnostic option. Many researches have already investigated various deep learning techniques, which have a significant impact on the quick and precise early detection of Covid-19. Most of the existing techniques, though, have not been trained and tested using a significant amount of data. In this paper, we purpose a deep learning technique enabled Convolutional Neural Network (CNN) to automatically diagnose Covid-19 from chest x-rays. To train and test our model, 10,293 x-rays, including 2875 x-rays of Covid-19, were collected as a data set. The applied dataset consists of three groups of chest x-rays: Covid-19, pneumonia, and normal patients. The proposed approach achieved 98.5% accuracy, 98.9% specificity, 99.2% sensitivity, 99.2% precision, and 98.3% F1-score. Distinguishing Covid-19 patients from pneumonia patients using chest x-ray, particularly for human eyes is crucial since both diseases have nearly identical characteristics. To address this issue, we have categorized Covid-19 and pneumonia using x-rays, achieving a 99.60% accuracy rate. Our findings show that the proposed model might aid clinicians and researchers in rapidly detecting Covid-19 patients, hence facilitating the treatment of Covid-19 patients.

## 1. Introduction

Wuhan, a business hub in China's Hubei province, witnessed the outbreak of a novel coronavirus in 2019. Chinese researchers termed the novel virus the 2019-novel-coronavirus (2019 n-Cov) or the Wuhan virus (Singhal, 2020). The global virus-knowledgeable community refers to it as CoronaVirus-2 Severe Acute Respiratory Syndrome (SARS-CoV-2) and even the 2019 epidemic coronavirus infection (Covid-19) (Lai et al., 2020; Li et al., 2020; Sharfstein et al., 2020). Coronaviruses have caused sickness in humans who have primarily been exposed to bats and rats as wild animals (Loey et al., 2020b; Rabi et al., 2020; York, 2020).

Covid-19 is a disease caused by an irresistible source that aggravates the lungs. Although RT-PCR testing (Wang et al., 2020b) is currently the most reliable method for identifying Covid-19 infection, it is a lengthy, hard, and complicated manual process, and there is an insufficient supply of testing kits. In addition, it involves nasopharyngeal swabs, which are uncomfortable for the patients while taking the sample.

In contrast, x-ray analysis can be an alternative appropriate method

because it involves low cost, has extensive range of applications, and offers rapid speed to detect COVID-19. Consequently, this approach can eliminate the problems related to RT-PCR testing. Utilizing x-ray image is essential for screening and diagnosing Covid-19 cases as Covid-19 targets human pulmonary epithelial cells and x-rays are a valuable tool for determining the health of a patient's lungs (Bassi and Attux, 2022; Ghose et al., 2021; Pham, 2021; Rahman et al., 2021; Wang et al., 2020a).

Without human interference, Convolutional Neural Networks (CNN) is capable to discover and derive characteristics and depict very complex nonlinear operations on its own. After a supervised training process, it operates solely based on input data. The ImageNet Large-Scale Visual Recognition Challenge (ILSVRC) reported a well-known scenario when a model outstripped human-level output in the task of classifying images in 2015 (He et al., 2015). Besides this, deep learning is also successfully applied in many sectors for its superior capability for automatic features extraction and outstanding performance, for example, human activity recognition (Cheng et al., 2022; Huang et al., 2021, 2022; Tang et al., 2022), the reconstruction of gene regulatory networks (Biswas et al.,

\* Corresponding author.

E-mail addresses: [parthoghosh92@gmail.com](mailto:parthoghosh92@gmail.com) (P. Ghose), [mdashrafuddin@students.federation.edu.au](mailto:mdashrafuddin@students.federation.edu.au) (Md.A. Uddin), [uzzal@cse.jnu.ac.bd](mailto:uzzal@cse.jnu.ac.bd) (U.K. Acharjee), [selina@cse.jnu.ac.bd](mailto:selina@cse.jnu.ac.bd) (S. Sharmin).

<https://doi.org/10.1016/j.iswa.2022.200130>

Received 31 May 2022; Received in revised form 19 September 2022; Accepted 22 September 2022

Available online 6 October 2022

2667-3053/© 2022 The Author(s). Published by Elsevier Ltd. This is an open access article under the CC BY license (<http://creativecommons.org/licenses/by/4.0/>).

2022), temporal forecasting of taxi flow (Lv et al., 2021b), and urban traffic visualization techniques (Lv et al., 2021a).

Many researchers (Biswas et al., 2022; Abdul Salam et al., 2021; Akter et al., 2021; Mahbub et al., 2022b) have already proposed CNN based Covid-19 detection approaches. For example, Akter et al. (2021) provided an automated classification approach based on deep learning and a Convolutional Neural Network that displays a quick COVID-19 detection rate. The training dataset includes of 3616 COVID-19 chest X-ray images and 10,192 healthy chest X-ray images. Abdul Salam et al. (2021) developed two machine learning models where one is a federated learning model and another is a standard machine learning model to show accuracy comparison to detect COVID-19 using a descriptive dataset and chest x-ray (CXR) images from COVID-19 patients. Agrawal and Choudhary (2022) proposed a deep convolutional neural network-based architecture for detecting COVID-19 utilizing chest radiographs. They used considerably large dataset and got a promising accuracy from their model. Biswas et al. (2022) collected a number of publicly available, unique COVID-19 x-ray and CT image datasets. They evaluated and compared the performance of their suggested 22-layer convolutional neural network model with ResNet-18, and VGG16.

This research aims to develop a paradigm based on deep learning for distinguishing Covid-19 patients from healthy and normal individuals by analyzing the presence of symptoms or x-ray abnormalities. We intend to provide a low-cost approach for radiologists and medical professionals to cross-check their interpretations and identify any potential outcomes that could otherwise be missed.

In addition, we designed a screening method so that it can assist the radiologists to easily identify the portions of the x-ray for Covid-19, bacterial or viral pneumonia, and normal peoples. We worked on the datasets newly generated by the radiological society, several sites such as kaggle, github, and other researchers. This dataset gave us the labeled data required to train and test our architecture for classification. Afterwards, we made two datasets (dataset-1 and dataset-2) from the collected x-rays. Dataset-1 contained three class x-ray images which is Covid-19, normal and pneumonia patients images whereas dataset-2 made up with Covid-19 and pneumonia images. The contributions of this paper can be summarised as follows:

- Collecting and pre-process x-ray data, build a CNN based architecture to recognize Covid-19 patient's x-ray.
- First, we trained our system to classify three class x-ray image. Utilizing our architecture, we can recognize chest x-ray images with an accuracy rate of 98.5% for 3 classes (Covid-19, normal, and pneumonia).
- For two class classification, we trained our model to differentiate Covid-19 sufferers from pneumonia patients which is very essential and critical. Our stated architecture showed good performance obtaining an accuracy of 99.60% on dataset-2.
- Finally, the Gradient Class Activation Map (Grad-CAM) technique was applied to locate typical features from x-rays to assist visually interpretive decision-making for detection cases.

The rest of the part of this paper is outlined as follows: In 2, literature review described while briefly discuss our problem statement in 3. Our proposed Covid-19 detection system's method is discussed in 4. Finally, showing the outcomes of the research in 5 and in 6, we summarized our research with some future research scopes.

## 2. Literature review

Recently many researchers have explored different deep learning approaches to identify Covid-19 using clinical data such as CT scans and x-rays. For instance, Alqudah et al. (2019) applied machine learning methods to construct a tool for classifying Covid-19 from chest x-rays. They applied several classification algorithms such as SVM and RF for categorizing x-ray images. They claimed 95.2% accuracy, 100%

specificity, and 93.3% sensitivity. The setback of this approach is that machine learning algorithms are not suitable for processing images like x-rays. For this reason, many deep learning approaches have been applied in the research to detect COVID-19 from images. To mention next, Loey et al. (2020b) suggested a generative adversarial network (GAN) to detect Covid-19 using x-ray. For Covid-19 identification purposes, the system explored three pre-trained models: GoogleNet, ResNeT18, and AlexNet. GoogleNet was chosen as the powerful DL technique within the four class cases, and the authors gained 80.% test accuracy for three-class classification. In contrast, AlexNet achieved an 84.3% accuracy rate in the three classes case, whereas GoogleNet achieved 99.4% test accuracy in the two classes scenario. However, their models were trained using a limited number of x-rays. Likewise, Horry et al. (2020) devised a deep learning model to identify Covid-19 using chest x-rays to be fed into pre-trained algorithms. For classifying x-rays, the recommended system utilized Inception, ResNet, Xception, VGG16, and VGG19. The dataset used by the model is generated by collecting 322 pictures of pneumonia patients, 115 images of Covid-19 cases, and 6162 images of ordinary individuals. Both the VGG16 and VGG19 classifiers have 80% sensitivity and accuracy which is not so promising for such sensitive infectious diseases.

Again, Bhattacharyya et al. (2022) established an approach to effectively distinguish Covid-19 patients from healthy persons using x-ray images. They performed segmentation on x-rays using deep learning based segmentation process before feeding the data into classification models to enhance outcomes. A conditional generative adversarial network (GAN) was applied to segment the lung image and trained using available ground truth masks by using a pixel-to-pixel approach. Finally, they used several ML algorithms, including softmax, RF, SVM, and XG Boost to classify the images. The accuracy of the VGG 19 architecture combined with the BRISK key-points mining approach with RF as the classification layer was 96.6%.

Ucar and Korkmaz (2020) introduced a deep CNN based Covid-19 detection system utilizing x-ray images. The dataset used for training the model included 1583 images of normal cases, 4290 images of pneumonia cases, and 76 images of Covid-19 cases and for Covid-19 cases and the model achieved 98.3% accuracy. However, the dataset is not significantly large enough to adopt the model in real life. Meanwhile, Apostolopoulos and Mpesiana (2020) also proposed a transfer learning technique by employing CNN. This approach might effectively recognize Covid-19 patients by analyzing key characteristics from chest x-rays. The method used five CNN models to categorize Covid-19 pictures, namely Inception, InceptionResNetV2, VGG19, Xception, and MobileNet. VGG19 was selected as the primary model for achieving the highest results (94.48% accuracy, 93.85% specificity, and 97.57% sensitivity). They used 700 images of pneumonia patients, 224 Covid-19 patients, and 504 images of ordinary people for the dataset.

In contrast, Bandyopadhyay and Dutta (2020) offered a completely new approach that employed the LSTM-GRU to characterize confirmed, discharged, negative cases, and death instances of Covid-19. The original system achieved 8% for confirmed cases, 67.8% accuracy for negative patients, 62% accuracy for death cases, and 40.5 percent accuracy for discharged cases. Khan et al. (2020) proposed an enhanced DL network to automatically detect Covid-19 instances via lung x-rays. This study used 1248 images as a dataset combining Covid-19 pneumonia viral, pneumonia bacterial, and ordinary individuals' x-ray images. The suggested approach achieved 93.5% accuracy, 97% precision, and 100% sensitivity in the situation of Covid-19.

To distinguish Covid-19 cases from normal cases using CT scans, Singh et al. (2020) applied a deep transfer learning model, VGG. In this approach, features are extracted using principal component analysis (PCA) for classification with four different classifiers. With a bagging ensemble approach and SVM classifier, the following performances metrics were found: 95.6% accuracy, 94.8% precision, and 96.3% F1-score. Similarly, Ahuja et al. (2021) suggested a transfer learning technique employing a three-phase approach. Several pre-trained

methods were fitted with an augmented image utilizing the ResNet18 model to indicate the irregularity of the image, resulting in 99.4% test case accuracy. [Alshazly et al. \(2021\)](#) exhibited a deep learning model trained using chest CT-scans to make this process more faster and automated. Several researchers have attempted to detect covid19 more reliable by combining multiple models. For example, [Aslan et al. \(2021\)](#) effectively merged two pre-trained Alexnet architectures (transfer learning and BiLSTM layer) for detecting Covid-19. They claimed that the proposed hybrid system shows higher Covid-19 detection accuracy than any single model. Furthermore, [Ter-Sarkisov \(2022\)](#) presented a COVID-CT-MaskNeT model to forecast Covid-19 using chest CT-scan images, and they obtained 90.80% sensitivity for Covid-19 cases, 91.62% sensitivity for Pneumonia cases, and a mean accuracy of 91.66% and an F1-score of 91.50% by training only a tiny proportion of the model's parameters.

Further, [Karthik et al. \(2021\)](#) implemented a customized CNN-based system to distinguish Covid-19 instances, and it can adopt distinct convolutional filter patterns for each type of pneumonia. To prevent epidemics and increase production in the [Lv et al. \(2021a\)](#) introduced a deep learning model. To predict the urban traffic revitalization index for the influential cities in China, they built DeepTRI using deep learning. Traveling is a big issue during pandemic. As a result, prediction of traveling demand considering environmental factors is a important factor and bare in mind this ([Xu et al., 2022](#)) presented a deep learning based traveling demand prediction system. Deep learning also is being successfully applied in many medical sectors. For example, PreRBP-TL is used for the reconstruction of gene regulatory networks and prediction of genomic properties such as accessible regions, chromatin connections, and TFBSs ([Biswas et al., 2022](#)) Researchers also have explored diverse kinds of system that can effectively detect Covid-19 individuals from chest x-rays. The above discussion reveals that deep learning, mainly Convolution Neural Network (CNN), plays a crucial role in recognizing and characterizing Covid-19 infection in medical imaging. Therefore, this study aims to explore deep learning to detect Covid-19 from the x-ray images. Several state-of-the-art works are briefly presented in [Table 1](#).

**Table 1**  
Studies evaluating DL methods for Covid-19 identification.

Study	Population	Models used	Accuracy (in %)
<a href="#">Loey et al. (2020a)</a>	760 CT-scans	CGAN, AlexNet, GoogleNet, VGGNet16, VGGNet19, ResNet50	82.9
<a href="#">Alshazly et al. (2021)</a>	2482 CT-scans	SqueezeNet, ResNet50, InceptionV3, ResNet101, ResNeXt50, ResNeXt101, Xception, DenseNet169, DenseNet201	93.7
<a href="#">Maghded et al. (2020)</a>	Real-time CT-Scan images	Smartphone, onboard sensors, ML models	N/A
<a href="#">Lahsaini et al. (2021)</a>	4986 CT-scans	DenseNet121, DenseNet201, VGG16, VGG19	97.8
<a href="#">Panwar et al. (2020)</a>	337 x-rays	nCOVnet	97.97
<a href="#">Aslan et al. (2021)</a>	2905 x-rays	mAlexNet BiLSTM (Hybrid) architecture	97.70
<a href="#">Purohit et al. (2022)</a>	5220 CT-scans	Deep Learning	96.47
<a href="#">Bassi and Attux (2022)</a>	2064 x-rays	Deep CNN	99.02
<a href="#">Mahbub et al. (2022a)</a>	1200 x-rays	Customized DNN	97.87
<a href="#">Gaur et al. (2021)</a>	3106 x-rays	EfficientNetB0, VGG16, InceptionV3	92.93

### 3. Problem statement

The Covid-19 virus, just like all the other bacteria or viruses, has been shown to cause pneumonia in some patients. However, the care of these cases is entirely different. If an individual is found sick, certain precautionary steps are taken in conjunction with the diagnosis. Precautionary step like keeping the patient under isolation for some days is required to underrate the risk of infecting someone in the case of the Covid-19 virus. It is also important to work out the distribution of the Covid-19 in different parts of the globe and take necessary measures to minimize the spread. Accurate and prompt detection of pneumonia caused by the Covid-19 virus is thus the greatest problem.

The WHO-approved coronavirus testing tool is the reverse transmission Polymerase chain reaction (RT-PCR) method, where the short DNA or RNA sequences are analyzed and replicated or intensified ([Corman et al., 2020](#)). To find out the possibility of the coronavirus, specific individuals need over one test. The WHO laboratory researchers establish that the negative findings in RT-PCR tests do not ignore the chance that the previously infected individuals may bare the virus with them ([Liu et al., 2020](#)). So, in this case, a quick test is required, which is possible by using an x-ray. Apart from this, the insufficient supply of Covid-19 scanning workstations and research kits poses a significant burden on medical practitioners and personnel to cope up with the problem. Rapid and effective identification of suspicious Covid-19 cases may be a big problem for physicians in this situation. The need for several checks using kits to ensure the proper infection status of patients and thus make acceptable decisions often occurs an exponential growth in situations.

Additionally, early identification of potential cases of Covid-19 is a concern as it includes public health protection and pandemic prevention. Any inability to detect the disease caused by the Covid-19 virus results in a rise in the risk of death. The amount of time that means the time between contracting the virus and starting to get disease signs is 1–14 days. This makes it really difficult to diagnose Covid-19 illness, accompanied by the individual's health conditions at a very preliminary phase. To overcome all these difficulties, diagnosis using x-ray could be a good alternative. The specific objectives are as follows:

- Helping radiologists and medical experts to identify the slit and slow changes among multiple x-rays, that otherwise could be overlooked.
- Due to the high expense of radiologist, many people in underdeveloped nations are unable to visit them. This tool might assist in the interpretation of chest x-ray as Covid-19, pneumonia, or normal.
- As Covid-19 and pneumonia is very similar disease in nature, so it could be difficult to distinguish them by human eyes. For this reason, we built and trained our model to classify covid-19 and pneumonia patients using x-ray as well.

### 4. Research methodology

This section presents the main contribution of the paper: the architectural design and development of proposed methodology. The main idea of the method proposed in this paper is to increase the accuracy of Covid-19 patient detection from the chest x-rays dataset.

#### 4.1. Methods and material

The artwork of the overall system for Covid-19 detection mainly consists of a number of phases as illustrated in [Fig. 1](#).

At fast, raw x-ray images are given in the pre-processing pipeline for performing pre-processing tasks like resizing, normalization, flipping, zooming, and rotation. After pre-processing phase, the data set was broken into training and test set. Then the train data is used for training the proposed architecture. After every epoch, the accuracy and loss of training and validation are determined. Subsequently, effectiveness was evaluated utilizing assessment metrics: confusion matrix, accuracy,

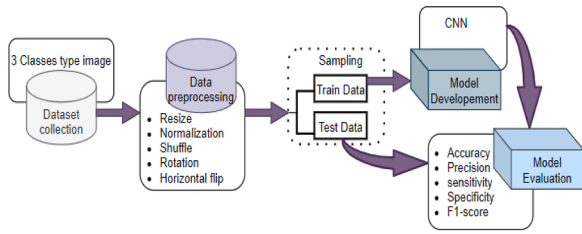


**Fig. 1.** The work flow of the introduced Covid-19 detection system includes: Data collection, data pre-processing, CNN model designed, and evaluation.

sensitivity, specificity, F1-score, precision, and AUC using ROC.

#### 4.1.1. Data collection and description

As Covid-19 very recently emerged, hardly any of the enormous archives include any Covid-19 tag data. As a result, we must rely on various imaging sources, including normal, pneumonia, and Covid-19 instances. For Covid-19 cases, 2875 x-ray pictures were gathered from the subsequent sites: GitHub (Cohen et al., 2020) and kaggle (Patel, 2020). For pneumonia and normal cases 4200 and 3218 x-ray images are taken from the Kaggle repository (Mooney, 2017; Patel, 2020). We gathered 10,293 x-ray pictures in total. After that, the images are reshaped to 224x224 pixel resolution. The depiction of some x-ray pictures of each class is depicted in Fig. 2.

We intended to make our model robust. With that intention, we make two dataset from the collected data and trained our model using both dataset. One (dataset-1) for three class combining Covid-19, normal and pneumonia patients x-ray images shown in Table 2 and other (dataset-2) for two class combining all the Covid-19 and pneumonia x-rays as mention in Table 3.

#### 4.1.2. Image pre-processing

Often pre-processing of the image is performed to enhance the efficiency of the model. In our job, we have also carried out certain pre-processing activities to produce better performance. The pre-processing techniques used in this research are listed in this section.

##### A.1 Resize Picture to Capture the Central Portion and Removing Black bars

Typically, CNN uses square images as details. Our chest x-ray data collection is obtained from various source data sets of different sizes. So, to feed the network, we'd have to change the scale of the photos to a square format. But as seen in the Fig. 3, it causes an asymmetry of the images.

In order to avoid removing the available data from the images, we wanted to avoid distortion of the input images. As a consequence, we used a technique introduced by Pasa et al. (2019) to remove the central area and delete black bars. The Fig. 4 depicted a pre-processed image

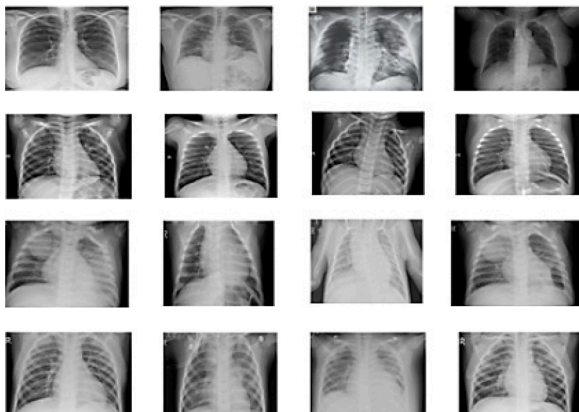


**Fig. 2.** Some x-ray images of the datasets.

**Table 2**

Dataset-1: Data set for three classes (Covid-19, normal and pneumonia patients).

Dataset	Normal	Covid	Pneumonia	Total
Train Set	2606	2300	3402	8308
Validation Set	290	288	378	956
Test Set	322	287	420	1029
Total	3218	2875	4200	10,293

**Table 3**

Dataset-2: Data set for two classes (Covid-19 and pneumonia patients x-rays).

Dataset	Covid-19	Pneumonia	Total
Train Set	2300	3402	5702
Validation Set	288	378	666
Test Set	287	420	707
Total	2875	4200	7075

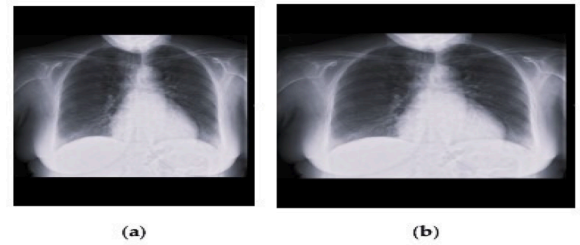


**Fig. 3.** Distortion due to the images being resized to a square shape. (a) Displays the original x-ray form of a COVID patient; (b) Displays the resampled image in a square shape.

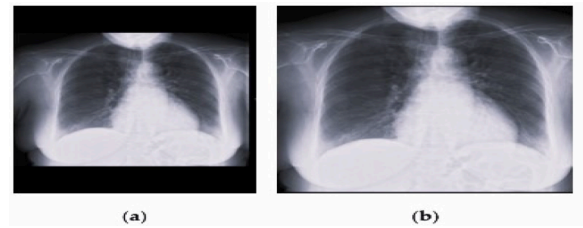


**Fig. 4.** Preprocessing is applied on all dataset files. (a) Displays the original x-ray of an individual with Covid-19 (b) Displays a square shape of the pre-processed image.

that carries out the following operations:

1. If at the margins of the image, any black band arises, then they are discarded.
2. Until about the minimum boundary counts 224 pixels, the dimension of the image is morphed.
3. Retrieve the 224x224 pixel core area.

##### A.2 Normalization

The photos were then standardized and transformed to the proper data format in the final stage. Individual pixels in the original images are stored as Unit8 type with values ranging from 0 to 255. Data in the float32 type must be given for the Keras model. As a result, the photos that were pre-processed must be transformed. It had also been scaled to a range of 0 to 1. To normalize the images, each pixel was divided by the maximum value of uint8, which is 255.

##### A.3 Data Augmentation

Deep-learning methods, such as CNN, also deliver favorable solutions if large number of images is used. As a consequence, data



augmentation is valuable in developing CNN based system. For this reason, at training time, we carried out the corresponding data augmentation operations:

- 5 to 10 degrees of spontaneous rotation.
- Zooming on an range about +10% and -10%.
- Flipping Horizontally.

#### 4.1.3. Proposed CNN model development

A system has been built in this paper to diagnose Covid-19 incidents systematically using three types of x-ray images. The suggested CNN model's architecture for Covid-19 detection is shown in the Fig. 5.

The proposed CNN model has five convolutional blocks. Each convolutional block has multiple layers and each layer has one activation function named Rectified linear unit (ReLU). The third block and fourth block has a dropout layer to reduce the over-fitting problem. Two fully connected layers (FCN) have been used, the first FCN is used with the dropout layer and last FCN layer is connected with the softmax classifier.

##### A.1 Convolution Layer

Every convolution block of this model has multiple convolution layers. The name of the first convolution block consists of conv1-layer1, conv1-layer2. Similarly second convolution block conv2-layer1, conv2-layer2, third convolution block conv3-layer1, conv3-layer2, fourth convolution block conv4-layer1, conv4-layer2, and final fifth block conv5-layer1, conv5-layer2. The fourth block and fifth block have an extra dropout layer to reduce the overfitting problem. Conv1 block has used a total of 32 filters where every filter size is 5 x 5. Conv2 block has used a total of 64 filters where every filter size is 3 x 3. Conv3 block has used a total of 128 filters where every filter size is 3 x 3. Conv4 block has used a total of 256 filters where every filter size is 3 x 3 and similarly, Conv5 block has used a total of 512 filters where every filter size is 3 x 3. The functional process performed by the convolutional layer is as:

$$\phi(x, y) = (I \times \beta)(x, y) = \sum \sum I(x+m, y+n) \beta(m, n) \quad (1)$$

where, the input matrix is represented with  $I$ , a 2D filter of size  $m \times n$  is denoted by  $\beta$  and  $\phi$  depict a 2D feature map's output.  $I \times \beta$  describes the operation of the convolutional layer.

##### A.2 Rectified Linear Unit

Each convolution layer has an activation function. Here this model used Rectified linear unit (ReLU) activation function. The ReLU layer is used in feature maps to increase nonlinearity. By maintaining the threshold value at zero, ReLU does the activation of the neurons. It is stated mathematically as follows:

$$\psi(\alpha) = \max(0, \alpha) \quad (2)$$

##### A.3 Zero Padding Layer

The application of this layer is to zeros to the left, right, top and bottom edges of an image. We have applied 1 x 1 zero padding during our work.

##### A.4 Pooling Layers

After the ReLU layer, we decide to apply a pooling layer. It is utilized to dynamically decrease the spatial size of the representation and furthermore, used to reduce the number of parameters and computation in the network. So, it ultimately helps to minimize the over fitting problem. Among different pooling system, the most common one, MAX pooling with filter size of  $2 \times 2$  is used in this research.

##### A.5 Dropout Layer

There are lots of ways of controlling the capacity of convolutional neural networks to prevent overfitting. Dropout layer (Srivastava et al., 2014) is one of the major regularization methods to prevent overfitting problems. During training time, the dropout layer randomly sets some neurons activation to zero and that neurons will not update their weights. While training, dropout is set neuron active with some probabilities, otherwise set it to zero. Due to dropout, some neuron doesn't learn all features. In the testing time, there is no dropout layer applied. Most of the time, the value of dropout ratio,  $p = 0.5$  is a comfortable default. Although this value also can be tuned during data validation.

##### A.6 Fully Connected Layer

Fully connected layers create a connection between every neuron in one layer to each other neuron in another layer. The layer basically takes an input image or objects and outputs an N-dimensional vector against this, where N is the number of given classes that the model or program has to choose from Chang et al. (2018). The working procedure of it is, like, it aspects at the output of the previous layer and determines which features mostly associate to a particular class. Fundamentally, a fully connected layer looks at what high-level features most strongly correlate to a specific class and has specific weights so that when we compute the products between the weights and the previous layer output, we get the classification value.

##### A.7 Softmax

The softmax function with loss (Chen et al., 2014) is a used which crushes a N-dimensional vector  $x$  of random real values to an N-dimensional vector ( $x$ ) of real values in the range from 0 to 1 that will sum upto 1. The function is as following equation 3:

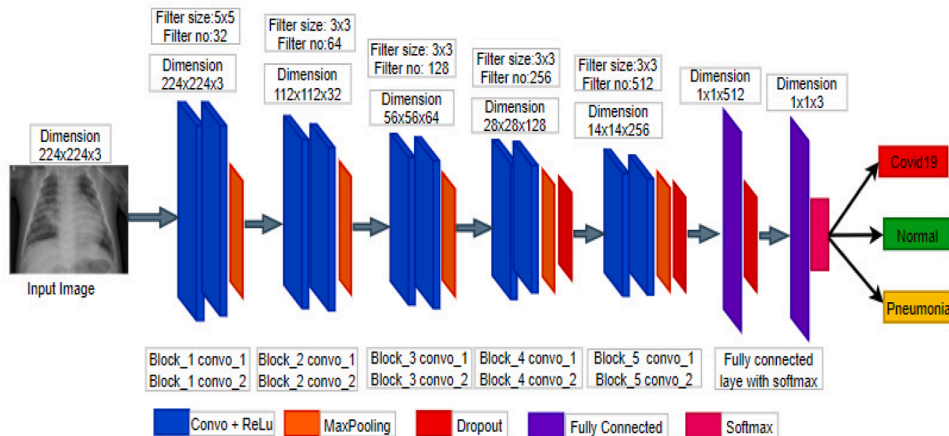


Fig. 5. Proposed CNN architecture with details layered view.

$$\sigma(x)_j = \frac{e_j^z}{\sum_{k=1}^k e_k^z} \quad (3)$$

Here,  $j=1,2,\dots,k$ . For this model, the output feature map, will be for 3 classes. In the output feature map the pixels belonging to the predicted class will be 1 and for that same pixel, other classes will contain zero.

#### 4.1.4. Cost sensitive learning

Our proposed method focuses on learning features automatically from x-ray images based on CNN. Cost-sensitive learning (CSL) (López et al., 2012) is a mechanism in which the method that ranks each class in a classification problem can be penalized. When using CNNs, CSL helps to prevent prejudice in classification. CSL then assists one as a tool to overcome the issue of imbalance. We have chosen it as our data set is imbalanced. In this analysis, the strategy of class weight is applied as one conceivable way while preparing to reduce the future effects of data imbalance. We change weights in the class weight system inversely related to class occurrences in the raw data. We have used a Sci-Kit Learn feature for all this, which acquires numbers to match the number of cases centered on logistic regression concepts. The weight  $W_k$  in class  $k$  is determined by the following Eq. (4).

$$W_k = \frac{\text{Total number of cases}}{\text{Number of classes} \times \text{Number of cases in class}(k)} \quad (4)$$

When matching the standard, the weights of the groups are used. Therefore, we allocate greater values to the cases of smaller groups in the loss function. The estimated loss would then be a weighted average, in which  $W_k$  is defined for the weights within each sample relating to each class during the loss calculation.

#### 4.1.5. Loss Function

The goal of network training is to maximize the probability of the actual class. This is gained by declining the cross-entropy loss for each training sample. The loss function used in our work is the categorical cross-entropy loss. In the following Eq. (5) categorical cross-entropy is specified.

$$\zeta(p, q) = - \sum W_k p_k \log(q_k) \quad (5)$$

where,  $k$  is the number of class used for training the model, and  $q$  is the Softmax function or predicted probability of class  $k$  and  $W_k$  is weight for class  $k$ .

#### 4.1.6. Screening and localizing pathogens

In order to better understand the stimulation of the last convolutionary layer of the developed model, we applied the Gradient-Weighted classes Activation Mapping (Grad-CAM) algorithm. The last convolutionary layer is the only one that delivers the parameters for the logistic layer of the final parameters to determine a probability distribution output. For constructing the Grad-CAM of an input file, the gradients of this layer have been used. Grad-CAM thus gives a coarse localization map that shows the most significant areas in the picture (radiological features).

## 5. Experimental results and discussion

In this section, we discussed the exploratory phase and assessment of the efficiency of the classification by the proposed architecture. The performances and the characteristics of our proposed system is also compared with existing works for Covid-19 detection.

### 5.1. Experimental process

The experimental details performed in this research are described in this section.

#### 5.1.1. Experimental environment

The proposed method is based on a learning rate of 0.001 with a 25 epoch number. The proposed CNN was introduced using Python along with the Keras package with the TensorFlow2 backend on the 1.80 GHz Intel(R) Core i5-8265U processor. Additionally, the tests were carried out using the GPU provided by google colab. We apply open CV for image pre-processing, matplotlib and seaborn for visualization graphs, sklearn for classification matrices, numpy and pandas.

#### 5.1.2. Split data into training set and testing set

We break the data into 90% for training images and 10% for testing which is 1029 images. We further break the training data by 10% for validation. We did this procedure for both dataset as mentioned in Tables 3 and 2. It was assured that the photographs were randomly divided between the test dataset and the train dataset, such that the two datasets were divided nearly evenly between the groups. It is also important that the model is educated in alternating categories. In other words, it would be over fitted, which is not desirable. Moreover, we perform five fold cross-validation to check the robustness of our model.

#### 5.1.3. Model training methodology

Adam optimizer was used to train every layer of the improvement parcel with the normal performance parameters ( $\beta_1 = 0.9$  and  $\beta_2 = 0.999$ ) using batches of size 32 and running throughout every epoch through the whole dataset. Eventually, adding an effective learning rate scheduler called "ReduceLROnPlateau" defines a lookup to control the relevance of the loss of reliability, starting with a learning rate of 0.001 on demand. After 5 epochs, we decreased the hyperparameter learning rate by a factor of 0.5, where improvement was not recorded by the detector. In the regularization section, in order to mitigate the consequences of over-learning, we have also put an early stop to discourage the over-learning of the network. Hyper parameters used in the proposed model are shown in the Table 4. We kept the parameters same for the binary classification(Covid-19 and pneumonia). For binary classification, we only changed the last dense layer to two instead of three.

### 5.2. Performance evaluation metrics

The results evaluation measures, including accuracy, precision, sensitivity, specificity, and F1-score, are used to assess the proposed system's performance. The performance evaluation metrics can be calculated as:

$$\text{Accuracy} = \frac{(\tau\rho + \tau\eta)}{(\tau\rho + \tau\eta + f\rho + f\eta)} \quad (6)$$

$$\text{Sensitivity} = \frac{\tau\rho}{(\tau\rho + f\eta)} \quad (7)$$

$$\text{Specificity} = \frac{\tau\eta}{(\tau\eta + f\rho)} \quad (8)$$

$$\text{Precision} = \frac{\tau\rho}{(\tau\rho + f\rho)} \quad (9)$$

**Table 4**

Hyper parameters of the network.

Hyper Parameter	Weight
Batch size	32
Cost function	Categorical Cross Entropy
Learning Rate (LR)	0.001
Learning Rate Multiplying factor	0.5
LR Decay	5 times after a plateau
Epochs	25
Optimizer	Adam

$$F1 - Score = \frac{2\tau\rho}{(2\tau\rho + f\rho + f\eta)} \quad (10)$$

where,  $\tau\rho$  = true positive;  $f\rho$  = false positive;  $\tau\eta$  = true negative and  $f\eta$  = false negative.

It is common to assess categorization results through schematic approaches such as the receiver operating characteristic curve (ROC curve) and its overall ranking, the area under the curve (AUC). As a result, we calculated the AUC ROC as well.

### 5.3. Results analysis

The details results of our stated model were discussed in this section. First, we trained our model applying dataset-1 (given in Table 2) to see how the stated model performs. Afterwards, we trained our model on dataset-2 (shown in Table 3) to check if our model was able to differentiate the Covid-19 and pneumonia cases correctly or not.

#### 5.3.1. Results for three class classification (Covid-19, normal, pneumonia):

The confusion matrix enables us to quantify metrics of our categorization task's results. The confusion matrix of the proposed CNN architecture for the test cases is shown in the Fig. 6.

Among the 1029 test images, our suggested approach misinterpreted only 44 images which indicate better and more consistent true positive and valid negative values. Therefore, the suggested CNN architecture can be used to correctly categorize Covid-19 instances.

In addition, the CNN classifier's performance is visually displayed in Figs. 7 and 8 in terms of accuracy and loss during the training and validation phases. For example, the training and validation accuracies at epoch number 25 are 98.6% and 97.8%, respectively. Furthermore, the suggested approach secures training and validation losses of 0.102 and 0.205, respectively.

The general accuracy, specificity, sensitivity, precision, and F1-score for every case of the proposed system are summarized in Table 5. The proposed CNN network has achieved 99.3% accuracy, 99.4% specificity, 99.0% sensitivity, 99.6% F1 score, and 98.0% precision for the Covid-19 cases. For normal patients, it had been recorded 99.2% accuracy, 99.6% specificity, 99.0% sensitivity, 99.0% precision, and 98.4% F1 score. The pneumonia cases have obtained 96.9% accuracy, 97.9% specificity, 99.0% sensitivity, 99.0% F1 score, and 98.2% precision. The best accuracy, specificity, and sensitivity were obtained within the normal cases. The best F1-Score and precision were detected within the pneumonia patients, along with the simplest specificity value.

Predict	Pneumonia	82	1	6
	Covid-19	1	232	19
	Normal	0	17	671
		Normal	Covid-19	Pneumonia
		Actual		

Fig. 6. Confusion Matrix for the proposed system for three class classification.

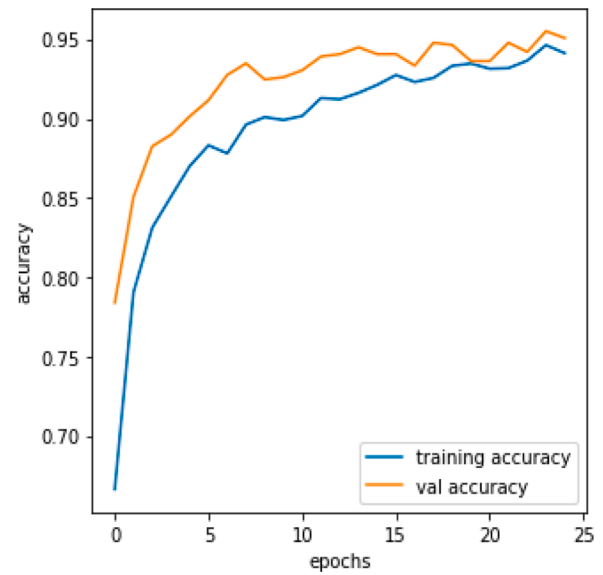


Fig. 7. Graph for Accuracy of the proposed system.

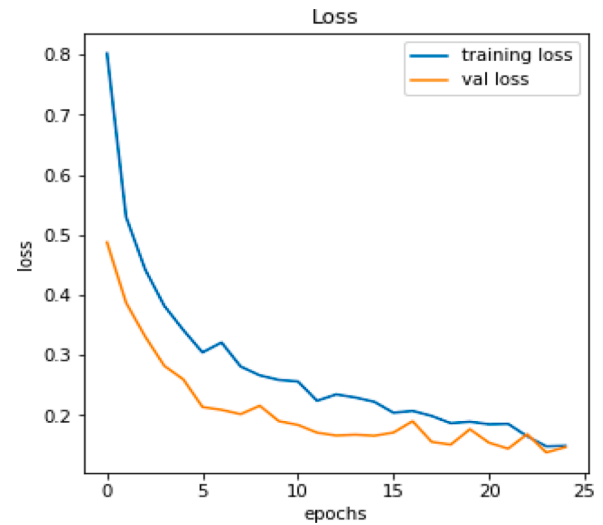


Fig. 8. Graph for Loss curve generated by the proposed system.

Table 5

Performance of the proposed network for classifying Covid-19, normal and pneumonia patient's x-ray images (in %).

Class	Accuracy	Specificity	Sensitivity	F1-Score	Precision
Covid19	99.3	99.4	99.0	99.6	98.0
Pneumonia	96.9	97.9	99.0	99.0	98.2
Normal	99.2	99.6	99.0	99.0	98.4
Average	98.5	98.9	99.0	98.3	99.2

Furthermore, ROC curves between the true positive and false-positive rates were generated to verify the overall performance, as illustrated in Fig. 9. For the recommended CNN architecture, the area under the ROC curve (AUC) was reported to be 96.6%.

Experimental findings show that the proposed architecture achieved the average AUC of 96%, 98.5% accuracy, 98.9% specificity, 99.0% sensitivity, 98.3% F1-score, and 99.2% precision for three cases classification.

In this study, our stated model had been compared to five different architectures. We kept the parameter same to train VGG16, VGG19,

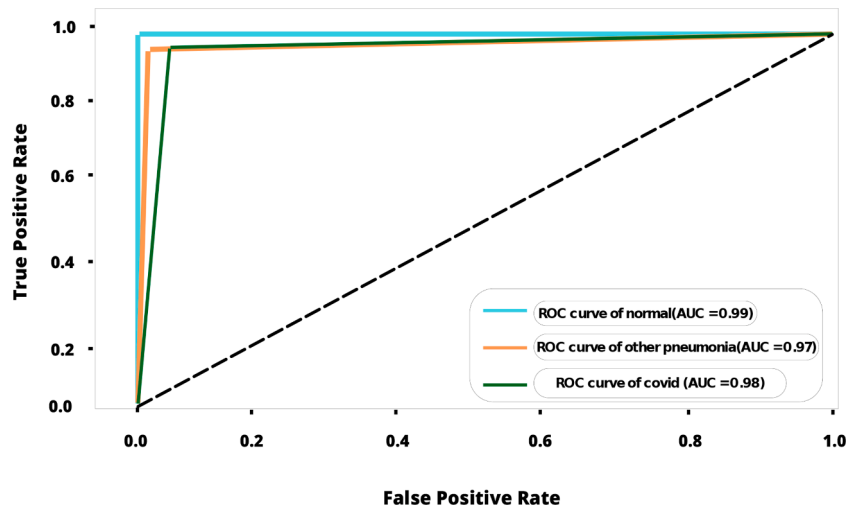


Fig. 9. ROC analysis of the developed work for dataset-1(covid, normal and pneumonia cases).

Xception, MobileNet and Inception-V2-Resnet on this dataset for valid comparison with our system.

Table 6 depicted the comparative performances of these model with our developed model taking the evaluation criteria accuracy, precision, specificity, sensitivity, and F1-Score. As demonstrated in Table 6, the suggested model also produced good performance in all the evaluation metrics with an accuracy of 98.5% on chest x-ray images.

### 5.3.2. Results for two class classification (Covid-19 and pneumonia cases):

The confusion matrix of the proposed CNN architecture for the dataset-2 is shown in the Fig. 10.

The confusion matrix indicates that our introduced deep learning model performed very well in precisely classifying Covid-19 patients from the pneumonia patients.

The accuracy, specificity, sensitivity, precision, and F1 score for Covid-19 and pneumonia case are summarized in Table 7. The proposed CNN network has achieved 99.8% accuracy, 99.9% specificity, 99.3% sensitivity, 99.7% F1 score, and 99.4% precision for the Covid-19 cases. Within the pneumonia cases, it has been found 99.2% accuracy, 99.9% specificity, 99.5% sensitivity, 99.9% precision and 99.2% F1 score.

Additionally, the ROC curves are generated between actual-positive-rate and the false-positive-rate with a view to determining the general performance shown in Fig. 11. For dataset-2, we obtained the region under the ROC curve (AUC) 99% for the proposed CNN architecture.

Again, to compare our introduced CNN model's performances, we have considered the VGG16, VGG19, Xception, MobileNet and Inception-V2-Resnet deep learning models and trained these using dataset-2. Table 8 depicted the comparative performances of these model with our developed model taking the evaluation criteria. As demonstrated in Table 8, the stated model again showed good

Predict	Covid -19	283	10
	Pneumonia	4	410
		Covid-19	Pneumonia
		Actual	

Fig. 10. Confusion Matrix of the stated system for covid and pneumonia classes.

Table 7

Performance of the proposed network to classify Covid-19 and pneumonia cases using Dataset-2(in %).

Class	Accuracy	Specificity	Sensitivity	F1-Score	Precision
Covid19	99.8	99.9	99.3	99.7	98.4
Pneumonia	96.2	99.9	99.5	99.2	98.2
Average	99.6	99.9	99.4	99.4	98.3

Table 6

Comparative analysis for three class classification results of the proposed and re-implemented deep CNN architectures in terms of performance metrics for dataset-1 (in %).

Class	Accuracy	Specificity	Sensitivity	F1-Score	Precision
VGG-16	95.2	100	93.3	92.0	90.0
VGG-19	95.0	96.0	95.0	95.0	95.0
MobileNet	95	97.5	96.9	95.6	95.0
Xception	90.0	93.5	90.7	90.4	91.2
Inception-V2-Resnet	94.72	96.46	98.66	91	91.5
Proposed System	98.5	98.9	99.0	98.3	99.3

performance in all the evaluation metrics with an accuracy of 99.6% for categorizing Covid-19 and pneumonia patients.

### 5.3.3. Results for 5-fold cross-validation:

We also have performed k-fold cross-validation to verify our proposed method's robustness and select k=5 in our experiment. The fold-wise results for 5-fold cross-validation are shown in Fig. 12 and Table 9. The confusion matrix and ROC curve depicted in Figs. 13 and 14 show our proposed model's robustness. Figure 3 shows that our proposed model achieves an average accuracy of around 97%, which is excellent for three classes. Again the ROC curve represents the outstanding



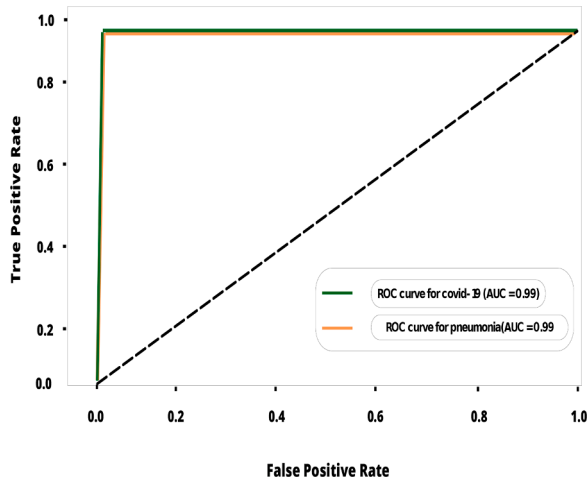


Fig. 11. ROC analysis for classifying covid and pneumonia patients applying dataset-2.

Table 8

Comparative analysis for two class classification results of the proposed and re-implemented deep CNN architectures in terms of performance metrics using dataset-2 (in %).

Class	Accuracy	Specificity	Sensitivity	F1-Score	Precision
VGG-16	97.2	98.3	96.3	96.0	5.0
VGG-19	97.0	97.0	96.0	97.0	95.0
MobileNet	98.1	97.8	97.9	96.5	97.3
Xception	96.0	92.0	95.0	96.0	91.0
Inception-V2-Resnet	90.0	89.0	90.0	90.0	83.0
<b>Proposed System</b>	<b>99.6</b>	<b>99.9</b>	<b>99.4</b>	<b>98.4</b>	<b>99.3</b>

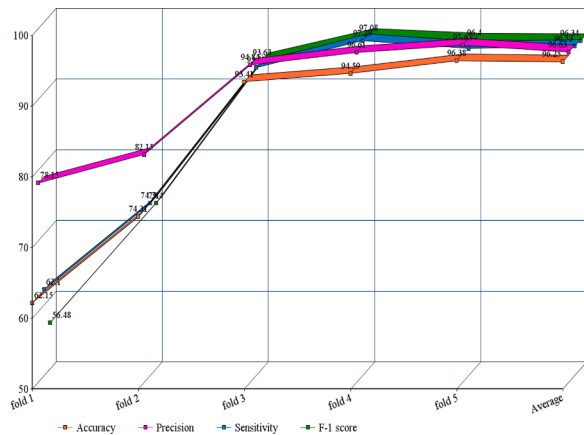


Fig. 12. Fold wise and average accuracy, precision, sensitivity and F-1 score.

Table 9

Performance of the proposed network on five-fold cross-validation(in %).

Class	Accuracy	Sensitivity	F1-Score	Precision
Fold1	62.15	62.10	56.48	78.15
Fold2	74.31	74.31	74.40	82.15
Fold3	93.41	93.51	93.63	94.84
Fold4	94.69	97.29	97.08	96.62
Fold5	96.38	96.38	96.40	97.63
Average	96.25	96.53	96.34	96.63

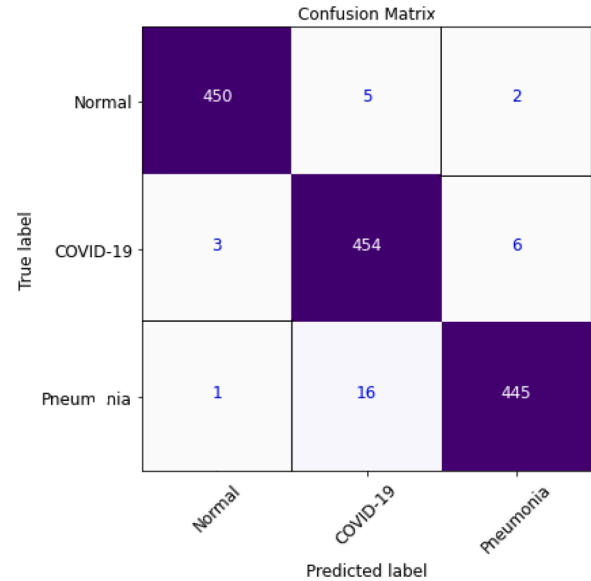


Fig. 13. Confusion Matrix for the proposed system on five-fold cross-validation.

performance of our introduced system, obtaining an average AUC of 99.45% and above 99% for Covid-19, pneumonia, and normal cases on five-fold cross-validation.

#### 5.3.4. Screening for pathogens

Gradient-weighted Class Activation Mapping (Grad-CAM) is often referred to as a heat map that is used the gradients of an identifying and mapping to dynamically view our test. In order to focus the significant portions within the image for forecasting, a rough localization map is generated after passing into the last layer. Of most important region (processed attributes) from which the classification decision has been made by the network reflects the deep blue colour. Fig. 15 shows the heat map for Covid-19, pneumonia, and normal cases of classified test samples.

The analysis of the results demonstrates that a CNN architecture plays an important effect on the detection of Covid-19 by supporting automated feature extraction from x-ray images. Our proposed system can extricate Covid-19 from pneumonia and normal cases with significant accuracy. Though it is tough to separate Covid-19 individuals from pneumonia patients, yet our proposed model is able to recognize Covid-19 showing good performances.

#### 5.4. Discussion and comparison with state-of-the-arts

As demonstrated in Tables 10 and 11, we assessed our model to other state-of-the-art Deep CNN techniques for recognizing Covid-19 on chest x-ray pictures. For the categorization of Covid-19 and other individuals pictures in our dataset, all of the algorithms in Tables 10 and 11 was re-implemented.

To identify Covid-19, paper (Bhattacharyya et al., 2022) employed VGG19 to extract semantic features with BRISK and used RF as a classifier in the output layer and discovered that the average accuracy, sensitivity, precision, and F1-Score was 96.6%, 95%, 95.0%, 95.0%, correspondingly. In Hussain et al. (2021), the researchers employed a transfer learning technique adopting MobileNet-v2 as a base model and obtained average classification accuracy, positive predictive value, and sensitivity of 99.12%, 99.27%, and 97.36%, respectively. Applying the transfer learning technique-based ResNet-34 model (Nayak et al., 2021), the authors obtained the accuracy, sensitivity, and precision of 95.29%, 92.97%, and 96.46%.

Correspondingly, the average classification accuracy, sensitivity, and

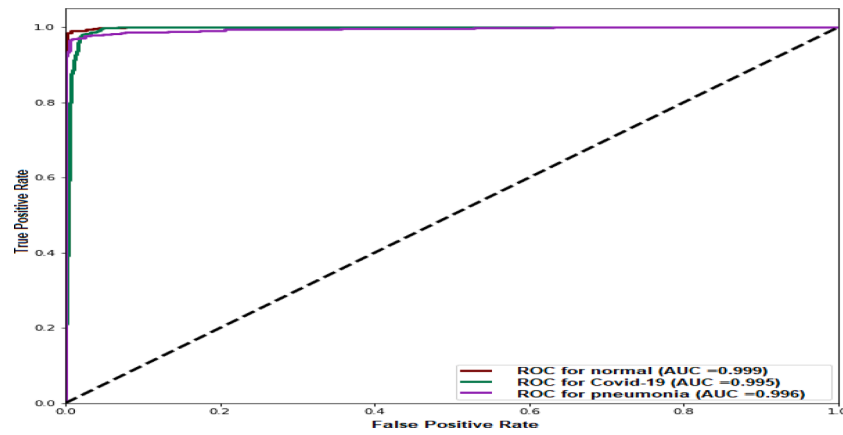


Fig. 14. ROC curve for the proposed system on five-fold cross-validation.

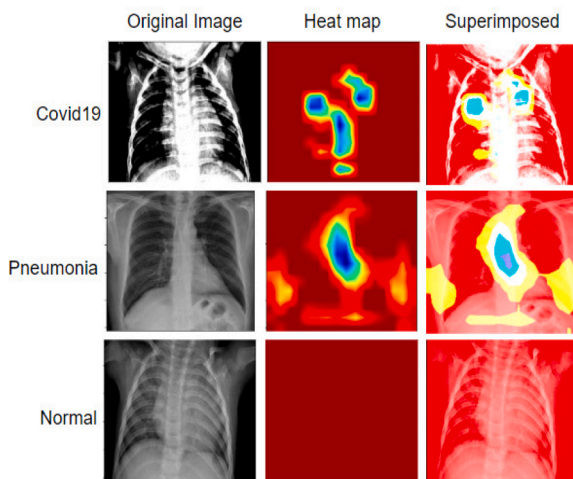


Fig. 15. Heat map image created by proposed CNN.

F1-score of a tuned AlexNet model (Pham, 2021) were 95.72%, 93.59%, and 96.78%. The researchers of Apostolopoulos and Mpesiana (2020), Khan et al. (2020), Ozturk et al. (2020), and Wang et al. (2020a) also tried to detect Covid-19 patients from x-rays using three types of x-ray: Covid-19, pneumonia and healthy individual's x-ray and they achieved more than 85% accuracy. In Rahman et al. (2021), the authors has proposed a novel DL model and obtained 97.65% accuracy, 100% precision, 95.59% recall, and 94.56% F1-Score. Table 10 proved that our suggested technique outstrips the recently developed Covid-19 identification techniques on chest x-rays.

At the same time, some researchers (Alqudah et al., 2019; Bhattacharyya et al., 2022; Mukherjee et al., 2021; Nayak et al., 2021; Pham, 2021) did their researches on identifying Covid-19 by applying two class

types images: Covid-19 versus pneumonia or Covid-19 versus normal as shown in Table 11. As per the table depicts, most of them did a tremendous job for classifying Covid-19 patients from others with a good accuracy scores. From the Table 11, it is clear that our stated model is absolutely comparable with the state-of-the-arts models for detecting Covid-19.

## 6. Conclusion

We built a deep CNN-based system to classify Covid-19, pneumonia, and healthy persons from x-ray pictures. CNN was used as a pattern identifier from the images for Covid-19 virus detection. The stated model can effectively differentiate other people from Covid-19 patients utilizing x-rays. The suggested framework achieved 98.5% accuracy, 98.9% specificity, 99.0% sensitivity, 99.2% precision, and 98.3% F1 score for three-class classification results. Furthermore, for two-class classification results, our stated architecture gained 99.6% accuracy, 99.60% specificity, 99.90% sensitivity, and 99.30% F1 score, which indicates that our model can effectively classify Covid-19 patients from pneumonia as well. Thus observing the results, it is clear that our designed architecture might be a better alternative for swiftly recognizing Covid-19 infection status and thereby halting the disease's development.

The proposed architecture's concept does have certain drawbacks. The use of limited data sets is the main shortcoming. As a result, in the future, we plan to perform additional tests with larger data sets and analyze the findings to improve our model's suitability and stability. We also intend to identify covid-19 patients suffers from other diseases. Furthermore, we want to train our model with other datasets like different cancerous datasets. We even want to associate the proposed model with radiologists who will be involved in future efforts.

Table 10

Comparison of the three class classification results of the introduced Covid-19 identification deep CNN model with others researches(in %).

Authors	Dataset	Accuracy	Specificity	Sensitivity	F1-Score	Precision
Pham (2021)	3314 x-rays	96.5	95.3	97.4	96.0	97.7
Bassi and Attux (2022)	2064 x-rays	98.02	-	98.82	-	99.92
Hussain et al. (2021)	400 x-rays	94.2	94.56	92.76	94.04	91.32
Sethy and Behera (2020)	381 x-rays	95.33	-	95.33	-	95.34
Khan et al. (2020)	924 x-rays	95.00	97.50	96.90	95.60	95.00
Apostolopoulos et al. (2020)	2855 x-rays	96.78	96.46	98.66	-	-
Sethy and Behera (2020)	381 x-rays	95.33	-	95.33	-	95.34
Wang et al. (2020a)	13,962 x-rays	93.3	-	-	-	-
Ozturk et al. (2020)	1127 x-rays	87.02	92.18	85.35	89.96	87.37
<b>Proposed System</b>	<b>10,293x-ray</b>	<b>98.5</b>	<b>98.9</b>	<b>99.0</b>	<b>99.2</b>	<b>98.3</b>

**Table 11**

Comparison of the two class classification results of the introduced Covid-19 identification deep CNN model with others researches(in %).

Authors	Dataset	Accuracy	Specificity	Sensitivity	F1-Score	Precision
Alqudah et al. (2019) <a href="#">Alqudah et al. (2019)</a>	67 x-rays	95.2	-	-	-	-
Nayak et al. (2021) <a href="#">Nayak et al. (2021)</a>	500 x-rays	95.29	-	96.46	92.97	97.5
A. Bhattacharyya et al. (2022) <a href="#">Bhattacharyya et al. (2022)</a>	930 x-rays	96.60	-	95.00	95.00	95.00
Pham (2021) <a href="#">Pham (2021)</a>	1314 x-rays	98.02	97.03	96.64	97.59	97.78
Ismael et al. (2021) <a href="#">Ismael and Şengür (2021)</a>	380 x-rays	94.70	97.89	97.78	94.00	95.92
Narin et al.(2021) <a href="#">Narin et al. (2021)</a>	14,194 x-rays	96.10	-	91.8	96.6	83.5
Mukherjee et al. (2021) <a href="#">Mukherjee et al. (2021)</a>	336 x-rays	95.83	-	97.31	98.21	93.45
Hussain et al. (2021) <a href="#">Hussain et al. (2021)</a>	800 x-rays	99.12	97.36	95.36	97.64	96.68
Rahman et al. (2021) <a href="#">Rahman et al. (2021)</a>	18,479 x-rays	95.11	95.59	94.56	94.55	94.53
Panwar et al. (2020) <a href="#">Panwar et al. (2020)</a>	284 x-rays	88	-	-	-	-
<b>Proposed System</b>	<b>7075 x-rays</b>	<b>99.60</b>	<b>99.90</b>	<b>99.00</b>	<b>99.40</b>	<b>99.30</b>

## CRediT authorship contribution statement

**Partho Ghose:** Conceptualization, Writing – original draft, Formal analysis, Methodology, Validation, Project administration. **Md. Ashraf Uddin:** Formal analysis, Methodology, Validation, Project administration. **Uzzal Kumar Acharjee:** Methodology, Validation, Project administration. **Selina Sharmin:** Formal analysis, Methodology, Validation, Writing – original draft.

## Declaration of Competing Interest

The authors declare that they have no known competing financial interests or personal relationships that could have appeared to influence the work reported in this paper

## References

- Abdul Salam, M., Taha, S., & Ramadan, M. (2021). Covid-19 detection using federated machine learning. *PloS one*, 16(6), 1–25.
- Agrawal, T., & Choudhary, P. (2022). Focuscovid: Automated covid-19 detection using deep learning with chest x-ray images. *Evolving Systems*, 13(4), 519–533.
- Ahuja, S., Panigrahi, B. K., Dey, N., Rajinikanth, V., & Gandhi, T. K. (2021). Deep transfer learning-based automated detection of covid-19 from lung ct scan slices. *Applied Intelligence*, 51(1), 571–585.
- Akter, S., Shamrat, F. J. M., Chakraborty, S., Karim, A., & Azam, S. (2021). Covid-19 detection using deep learning algorithm on chest x-ray images. *Biology*, 10(11), 1174.
- Alqudah, A. M., Qazan, S., Alquran, H., Qasmieh, I. A., & Alqudah, A. (2019). Covid-2019 detection using x-ray images and artificial intelligence hybrid systems. *Biomedical Signal and Image Analysis and Project: Biomedical Signal and Image Analysis and Machine Learning Lab: Boca Raton, FL, USA*.
- Alshazly, H., Linse, C., Barth, E., & Martinetz, T. (2021). Explainable covid-19 detection using chest ct scans and deep learning. *Sensors*, 21(2), 455.
- Apostolopoulos, I. D., & Mpesiana, T. A. (2020). Covid-19: Automatic detection from x-ray images utilizing transfer learning with convolutional neural networks. *Physical and Engineering Sciences in Medicine*, 1.
- Aslan, M. F., Unlarsen, M. F., Sabanci, K., & Durdu, A. (2021). Cnn-based transfer learning–bilstm network: A novel approach for covid-19 infection detection. *Applied Soft Computing*, 98, 106912.
- Bandyopadhyay, S. K., & Dutta, S. (2020). Machine learning approach for confirmation of covid-19 cases: Positive, negative, death and release. *medRxiv*.
- Bassi, P. R., & Attux, R. (2022). A deep convolutional neural network for covid-19 detection using chest x-rays. *Research on Biomedical Engineering*, 38(1), 139–148.
- Bhattacharyya, A., Bhaik, D., Kumar, S., Thakur, P., Sharma, R., & Pachori, R. B. (2022). A deep learning based approach for automatic detection of covid-19 cases using chest x-ray images. *Biomedical Signal Processing and Control*, 71, 103182.
- Biswas, M., Ghose, P., Alavi, M., Tabassum, M., Ashraf Uddin, M., Mahbub, K., Gaur, L., Mallik, S., & Zhao, Z. (2021). Detecting covid-19 infection status from chest x-ray and ct scan via single transfer learning-driven approach. *Frontiers in Genetics*, 2490.
- Chang, P., Grinband, J., Weinberg, B., Bardis, M., Khy, M., Cadena, G., Su, M.-Y., Cha, S., Filippi, C., Bota, D., et al. (2018). Deep-learning convolutional neural networks accurately classify genetic mutations in gliomas. *American Journal of Neuroradiology*, 39(7), 1201–1207.
- Chen, L.-C., Papandreou, G., Kokkinos, I., Murphy, K., & Yuille, A. L. (2014). Semantic image segmentation with deep convolutional nets and fully connected crfs. *arXiv preprint arXiv:1412.7062*.
- Cheng, X., Zhang, L., Tang, Y., Liu, Y., Wu, H., & He, J. (2022). Real-time human activity recognition using conditionally parametrized convolutions on mobile and wearable devices. *IEEE Sensors Journal*, 22(6), 5889–5901.
- Cohen, J. P., Morrison, P., & Dao, L. (2020). Covid-19 image data collection. *arXiv* 2003.11597.
- Corman, V. M., Landt, O., Kaiser, M., Molenkamp, R., Meijer, A., Chu, D. K., Bleicker, T., Brünink, S., Schneider, J., Schmidt, M. L., et al. (2020). Detection of 2019 novel coronavirus (2019-ncov) by real-time rt-pcr. *Eurosurveillance*, 25(3), 2000045.
- Gaur, L., Bhatia, U., Jhanjhi, N., Muhammad, G., & Masud, M. (2021). Medical image-based detection of covid-19 using deep convolution neural networks. *Multimedia Systems*, 1–10.
- Ghose, P., Acharjee, U. K., Islam, M. A., Sharmin, S., & Uddin, M. A. (2021). Deep viewing for covid-19 detection from x-ray using cnn based architecture. *2021 8th international conference on electrical engineering, computer science and informatics (eeeci)* (pp. 283–287). IEEE.
- He, K., Zhang, X., Ren, S., & Sun, J. (2015). Delving deep into rectifiers: Surpassing human-level performance on imagenet classification. *Proceedings of the IEEE international conference on computer vision* (pp. 1026–1034).
- Horry, M. J., Paul, M., Ulhaq, A., Pradhan, B., Saha, M., Shukla, N., et al. (2020). X-Ray image based covid-19 detection using pre-trained deep learning models. *engrXiv*.
- Huang, W., Zhang, L., Gao, W., Min, F., & He, J. (2021). Shallow convolutional neural networks for human activity recognition using wearable sensors. *IEEE Transactions on Instrumentation and Measurement*, 70, 1–11.
- Huang, W., Zhang, L., Wu, H., Min, F., & Song, A. (2022). Channel-equalization-har: A light-weight convolutional neural network for wearable sensor based human activity recognition. *IEEE Transactions on Mobile Computing*.
- Hussain, E., Hasan, M., Rahman, M. A., Lee, I., Tamanna, T., & Parvez, M. Z. (2021). Corodet: A deep learning based classification for covid-19 detection using chest x-ray images. *Chaos, Solitons & Fractals*, 142, 110495.
- Ismael, A. M., & Şengür, A. (2021). Deep learning approaches for covid-19 detection based on chest x-ray images. *Expert Systems with Applications*, 164, 114054.
- Karthik, R., Menaka, R., & Hariharan, M. (2021). Learning distinctive filters for covid-19 detection from chest x-ray using shuffled residual cnn. *Applied Soft Computing*, 99, 106744.
- Khan, A. I., Shah, J. L., & Bhat, M. M. (2020). Coronet: A deep neural network for detection and diagnosis of covid-19 from chest x-ray images. *Computer Methods and Programs in Biomedicine*, 105581.
- Lahsaini, I., Daho, M. E. H., & Chikh, M. A. (2021). Deep transfer learning based classification model for covid-19 using chest ct-scans. *Pattern Recognition Letters*, 152, 122–128.
- Lai, C.-C., Shih, T.-P., Ko, W.-C., Tang, H.-J., & Hsueh, P.-R. (2020). Severe acute respiratory syndrome coronavirus 2 (sars-cov-2) and corona virus disease-2019 (covid-19): The epidemic and the challenges. *International Journal of Antimicrobial Agents*, 105924.
- Li, J., Li, J. J., Xie, X., Cai, X., Huang, J., Tian, X., & Zhu, H. (2020). Game consumption and the 2019 novel coronavirus. *The Lancet Infectious Diseases*, 20(3), 275–276.
- Liu, W.-j. W., Yuan, C., Yu, M.-l., Li, P., & Yan, J.-b. (2020). Detection of novel coronavirus by rt-pcr in stool specimen from asymptomatic child, china. *Emerging Infectious Diseases Journal*.
- Loey, M., Manogaran, G., & Khalifa, N. E. M. (2020a). A deep transfer learning model with classical data augmentation and cgan to detect covid-19 from chest ct radiography digital images. *Neural Computing and Applications*, 1–13.
- Loey, M., Smarandache, F., & M Khalifa, N. E. (2020b). Within the lack of chest covid-19 x-ray dataset: A novel detection model based on gan and deep transfer learning. *Symmetry*, 12(4), 651.
- López, V., Fernández, A., Moreno-Torres, J. G., & Herrera, F. (2012). Analysis of preprocessing vs. cost-sensitive learning for imbalanced classification. open problems on intrinsic data characteristics. *Expert Systems with Applications*, 39(7), 6585–6608.
- Lv, Z., Li, J., Dong, C., Li, H., & Xu, Z. (2021a). Deep learning in the covid-19 epidemic: A deep model for urban traffic revitalization index. *Data & Knowledge Engineering*, 135, 101912.
- Lv, Z., Li, J., Dong, C., & Xu, Z. (2021b). Deepstf: A deep spatial–temporal forecast model of taxi flow. *The Computer Journal*.
- Maghdad, H. S., Ghafoor, K. Z., Sadiq, A. S., Curran, K., Rawat, D. B., & Rabie, K. (2020). A novel ai-enabled framework to diagnose coronavirus covid-19 using smartphone embedded sensors: design study. *2020 IEEE 21st international conference on information reuse and integration for data science (iri)* (pp. 180–187). IEEE.
- Mahbub, M. K., Biswas, M., Gaur, L., Alenezi, F., & Santosh, K. (2022a). Deep features to detect pulmonary abnormalities in chest x-rays due to infectious diseases: Covid-19, pneumonia, and tuberculosis. *Information Sciences*, 592, 389–401.

- Mahbub, M. K., Zamil, M. Z. H., Miah, M. A. M., Ghose, P., Biswas, M., & Santosh, K. (2022b). Mobapp4infectiousdisease: Classify covid-19, pneumonia, and tuberculosis. 2022 *IEEE 35th international symposium on computer-based medical systems (cbms)* (pp. 119–124). IEEE.
- Mooney, P. (2017). Chest x-ray images (pneumonia). <https://www.kaggle.com/paultimothymooney/chest-xray-pneumonia>.
- Mukherjee, H., Ghosh, S., Dhar, A., Obaidullah, S. M., Santosh, K., & Roy, K. (2021). Deep neural network to detect covid-19: One architecture for both ct scans and chest x-rays. *Applied Intelligence*, 51(5), 2777–2789.
- Narin, A., Kaya, C., & Pamuk, Z. (2021). Automatic detection of coronavirus disease (covid-19) using x-ray images and deep convolutional neural networks. *Pattern Analysis and Applications*, 24(3), 1207–1220.
- Nayak, S. R., Nayak, D. R., Sinha, U., Arora, V., & Pachori, R. B. (2021). Application of deep learning techniques for detection of covid-19 cases using chest x-ray images: A comprehensive study. *Biomedical Signal Processing and Control*, 64, 102365.
- Ozturk, T., Talo, M., Yildirim, E. A., Baloglu, U. B., Yildirim, O., & Acharya, U. R. (2020). Automated detection of covid-19 cases using deep neural networks with x-ray images. *Computers in Biology and Medicine*, 103792.
- Panwar, H., Gupta, P., Siddiqui, M. K., Morales-Menendez, R., & Singh, V. (2020). Application of deep learning for fast detection of covid-19 in x-rays using ncovnet. *Chaos, Solitons & Fractals*, 109944.
- Pasa, F., Golkov, V., Pfeiffer, F., Cremers, D., & Pfeiffer, D. (2019). Efficient deep network architectures for fast chest x-ray tuberculosis screening and visualization. *Scientific Reports*, 9(1), 1–9.
- Patel, P. (2020). Chest x-ray images (pneumonia). <https://www.kaggle.com/prashant268/chest-xray-covid19-pneumonia>.
- Pham, T. D. (2021). Classification of covid-19 chest x-rays with deep learning: New models or fine tuning? *Health Information Science and Systems*, 9(1), 1–11.
- Purohit, K., Kesarwani, A., Ranjan Kisku, D., & Dalui, M. (2022). Covid-19 detection on chest x-ray and ct scan images using multi-image augmented deep learning model. *Proceedings of the seventh international conference on mathematics and computing* (pp. 395–413). Springer.
- Rabi, F. A., Al Zoubi, M. S., Kasasbeh, G. A., Salameh, D. M., & Al-Nasser, A. D. (2020). Sars-cov-2 and coronavirus disease 2019: What we know so far. *Pathogens (Basel, Switzerland)*, 9(3), 231.
- Rahman, T., Khandakar, A., Qiblawey, Y., Tahir, A., Kiranyaz, S., Kashem, S. B. A., Islam, M. T., Al Maadeed, S., Zughaier, S. M., Khan, M. S., et al. (2021). Exploring the effect of image enhancement techniques on covid-19 detection using chest x-ray images. *Computers in Biology and Medicine*, 132, 104319.
- Sethy, P. K., & Behera, S. K. (2020). Detection of coronavirus disease (covid-19) based on deep features. *Preprints*, 2020030300, 2020.
- Sharfstein, J. M., Becker, S. J., & Mello, M. M. (2020). Diagnostic testing for the novel coronavirus. *JAMA*, 323(15), 1437–1438.
- Singh, M., Bansal, S., Ahuja, S., Dubey, R. K., Panigrahi, B. K., & Dey, N. (2020). Transfer learning based ensemble support vector machine model for automated covid-19 detection using lung computerized tomography scan data. *Research Square*.
- Singhal, T. (2020). A review of coronavirus disease-2019 (covid-19). *The Indian Journal of Pediatrics*, 1–6.
- Srivastava, N., Hinton, G., Krizhevsky, A., Sutskever, I., & Salakhutdinov, R. (2014). Dropout: A simple way to prevent neural networks from overfitting. *The Journal of Machine Learning Research*, 15(1), 1929–1958.
- Tang, Y., Zhang, L., Min, F., & He, J. (2022). Multi-scale deep feature learning for human activity recognition using wearable sensors. *IEEE Transactions on Industrial Electronics*.
- Ter-Sarkisov, A. (2022). Covid-ct-mask-net: Prediction of covid-19 from ct scans using regional features. *Applied Intelligence*, 1–12.
- Ucar, F., & Korkmaz, D. (2020). Covidiagnosis-net: Deep bayes-squeezenet based diagnostic of the coronavirus disease 2019 (covid-19) from x-ray images. *Medical Hypotheses*, 109761.
- Wang, L., Lin, Z. Q., & Wong, A. (2020a). Covid-net: A tailored deep convolutional neural network design for detection of covid-19 cases from chest x-ray images. *Scientific Reports*, 10(1), 1–12.
- Wang, W., Xu, Y., Gao, R., Lu, R., Han, K., Wu, G., & Tan, W. (2020b). Detection of sars-cov-2 in different types of clinical specimens. *JAMA*, 323(18), 1843–1844.
- Xu, Z., Lv, Z., Li, J., Sun, H., & Sheng, Z. (2022). A novel perspective on travel demand prediction considering natural environmental and socioeconomic factors. *IEEE Intelligent Transportation Systems Magazine*.
- York, A. (2020). Novel coronavirus takes flight from bats? *Nature Reviews Microbiology*, 18(4), 191–191.